Photovoltaic Cell Operating Temperature Models: A Review of Correlations and Parameters

Leticia de Oliveira Santos, Paulo Cesar Marques de Carvalho, and Clodoaldo de Oliveira Carvalho Filho

***Abstract*—A review of photovoltaic (PV) cell operating temperature (T_c) steady-state models developed from the year 2000 onward is shown in the present article. The goal is to help researchers and professionals in the field to choose the most significant parameters and suitable experimental arrangements to compose an accurate steady-state model. Initially, a brief description of T_c is given and an overview of the models for calculating T_c is presented. We present a summary of 33 correlations found in the literature for estimating T_c and the synthesis of those correlations in three general forms. Additionally, we highlight the main parameters in the analyzed correlations along with their most accurate data collection methods. The parameters with the greatest influence on T_c, appearing in a significant number of formulations, are discussed: solar absorbance, electrical efficiency, and transmittance of the PV cell/module glass cover; irradiance; ambient temperature; wind speed. Strategies of obtaining T_c—using the module back side temperature or an internal sensor for direct measurement—for model validation purposes are also discussed.**

***Index Terms*—Model selection, photovoltaic (PV) cell correlations, PV cell temperature, PV modules thermal models, performance prediction.**

Nomenclature

C_g	Geometric concentration ratio of the module.
FF	Fill factor.
G	Solar irradiance.
G_{NOCT}	Reference solar irradiance in NOCT conditions (800 W/m^2).
G_{ref}	Reference solar irradiance at STC conditions (1000 W/m^2).
I_{sc}	Short circuit current.
I_{scr}	I_{sc} of module at reference conditions.
k	Boltzmann's constant.
n	Empirically determined cell "diode factor".
p	Packing factor of solar module.
P_{max}	Maximum power.
q	Elementary charge.
Q_g	Radiation energy absorbed by the glass cover.
r	Ross coefficient.
T_a	Ambient temperature.
$T_{a,NOCT}$	Reference ambient temperature at NOCT conditions of 20 °C.
T_b	Module back side temperature.
T_c	PV cell operating temperature.
$T_{c,NOCT}$	PV cell operating temperature at NOCT conditions.
T_{ground}	Ground temperature.
$T_{h,0}$	Heat-sink temperature at shutter initiation.
T_{sky}	Sky temperature.
T_{STC}	Ambient temperature at STC conditions (25 °C).
U_L	Heat loss coefficient.
$U_{L,NOCT}$	Heat loss coefficient at NOCT conditions.
V_{max}	Maximum measured Voc for shutter event.
V_{oc}	Open circuit voltage.
V_{ocr}	V_{oc} of module at reference conditions.
V_w	Wind speed.
$V_{w,NOCT}$	Reference average wind speed at NOCT conditions of 1 m/s.

Abbreviations

BIPV	Building-integrated photovoltaics.
CFD	Computational fluid dynamics.
EVA	Ethylene vinyl acetate.
HCPV	High concentrating photovoltaic.
I-V curve	Current-voltage characteristic curve.
NOCT	Nominal operating cell temperature.
NTE	Nominal terrestrial environment.
OC	Open circuit.
PV	Photovoltaic.
SC	Short circuit.
STC	Standard test conditions.

Greek Letters

η	Electrical efficiency.
η_{STC}	Efficiency coefficient at maximal power under STC conditions.
β	Module Voc temperature coefficient.
β_{STC}	β at maximal power under STC.
τ	Coefficient of transmissivity.
α	Coefficient of absorbance.

I. Introduction

DESIGNING a photovoltaic (PV) system involves estimating its electricity production. Thereunto, the PV

Manuscript received June 24, 2021; revised August 24, 2021; accepted September 6, 2021. Date of publication October 22, 2021; date of current version December 23, 2021. This work was supported in part by CAPES and in part by CNPq. *(Corresponding author: Leticia de Oliveira Santos.)*

Leticia de Oliveira Santos and Clodoaldo de Oliveira Carvalho Filho are with the Department of Mechanical Engineering, Federal University of Ceará, Fortaleza, CE 60020-181, Brazil (e-mail: leticia@fisica.ufc.br; clodoaldo@ufc.br).

Paulo Cesar Marques de Carvalho is with the Department of Eletrical Engineering, Federal University of Ceará, Fortaleza, CE 60020-181, Brazil (e-mail: carvalho@dee.ufc.br).

Color versions of one or more figures in this article are available at https://doi.org/10.1109/JPHOTOV.2021.3113156.

Digital Object Identifier 10.1109/JPHOTOV.2021.3113156

performance must be considered, which is influenced by the environmental conditions and the resulting PV cell operating temperature (T_c) [1]. Therefore, a thermal model is necessary to estimate the PV operating temperature. However, designing, implementing, and effectively monitoring PV plants performance is a difficult task due to the influence of factors related to the physics of solar cells and the environment. Forecast models performances are affected by many elements of uncertainties, and the influence of the prediction methodology and model parameters on the final error is not clear [2]. A performance model is expected to identify and quantify the influence of all significant factors, including electrical, thermal, spectral, solar, and optical effects [3].

The models for T_c estimation can be basically classified by two approaches: steady state and dynamic. The main difference between the methodologies is that in the steady-state approach all parameters are assumed to be time-independent, while in the dynamic approach some parameters are time-dependent [4].

Steady-state models are relatively simple, characterized by low computing times; nevertheless, these models are not flexible and can overestimate or underestimate the value of T_c [5]. The intensity of incoming solar irradiance and other parameters that affect the PV modules performance, in a short period of time, are supposed to be constant. For instance, if the heat transfer variation between the PV module and the surroundings is low, it can be considered as steady-state condition; temperatures in different positions of the PV module are also considered constant for steady-state condition [6].

Dynamic models can express more realistic and precise results considering the fluctuation of the solar irradiance in a short period [6]; this technique is based on T_c determination using an energy balance [1]. Hence, dynamic models describe T_c and its thermal process in more details compared to steady-state models. Nevertheless, these models are relatively complex, requiring more computation time, cost, and effort [5].

In recent years, considerable efforts have been devoted by the scientific community to the development and improvement of approaches for T_c calculation from measurable parameters; in such process, steady state models for T_c determination have become common. Hence, in the present article, we review PV operating temperature steady-state models from the year 2000 onward, aiming to help researchers and professionals in the field to choose the most appropriate parameters and experimental arrangements to compose an accurate model. Additionally, we summarize 33 equations found in the literature for estimating T_c in just three general forms. According to our review, no similar approach was proposed previously, highlighting the original contribution.

The rest of this article is organized as follows: In Section II, we discuss the importance of T_c and present an overview of the calculation methods. In Section III, we analyze correlations found in the literature survey and present the three general forms that can express all the correlations considered in this review. In Section IV, we focus on the main parameters of the considered models, discussing the significant parameters for an accurate model development: PV module electrical efficiency, solar absorption, and glass cover transmittance; solar irradiance (G); ambient temperature (T_a); wind speed (V_w). In Section V, we comment strategies of obtaining T_c for model validation purposes and Section VI, concludes this article.

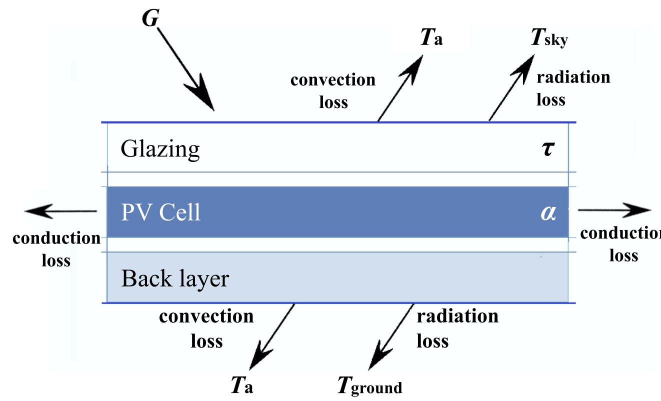

Fig. 1. Thermal processes in a PV module. Adapted from [10].

II. Thermal Models of PV Cell Operating Temperature

The T_c is fundamental to characterize the module's behavior, but it is not an easily available parameter [7]. Hence, in the scientific literature, a significant number of contributions demonstrating the adverse effect of an increase in T_c on the module performance can be found [8]. This adverse effect results from the decrease of PV cell energy interval (bandgap) when the temperature increases, implying a change in the cell electric behavior: open-circuit voltage (V_{oc}), efficiency (η), fill factor (FF), and maximum power (P_{max}) decrease; a negligible increase of the short circuit current (I_{sc}) occurs [9].

The thermal environment that establishes the instantaneous value of T_c is quite complex. A procedure that leads to the estimation of T_c is based on the energy balance of the module, which should consider both internal processes that occur during the bombardment of photons on the semiconductor, resulting in production of electricity, and not converted energy release as heat by standard mechanisms of heat transfer such as convection and radiation [10]. In most cases, these mechanisms affect the module front and back side, since in typical installations a distance between the module and the roof/slab is usually left to facilitate the rejected heat removal, allowing the module to operate in an efficient way. In the case of free-standing arrays, also should be considered the heat conduction through the mounting frame structure: heat is transported to the surfaces by conduction, and the surfaces release it to the environment by convection and radiation (see Fig. 1) [11].

In summary, T_c depends on factors such as: solar absorption properties of the cells; modules constituent materials (semiconductors, cells, layers, encapsulant, among others); thermal dissipation to the environment; installation and environmental conditions (location, G, T_a, and V_w) [12], [13].

The T_c prediction is the last step before reaching the power forecasting possibility [14]. The correlations for T_c found in the literature usually describe free-standing PV arrays, PV/thermal collectors, and building-integrated photovoltaics (BIPV) installations [4], [15]. These correlations express T_c as a function of the relevant meteorological variables and include material and system-dependent properties and parameters depending on the type of assembly arrangements/schemes. Some correlations express the adverse effect of an increasing T_c on η [16], [17]. Methods based on electrical parameters consider that parameters such as V_{oc} vary with temperature, allowing estimating T_c with the help of electrical data measurements, using different procedures [18].

In general, most correlations include a reference state and corresponding values of the significant variables. A method to formulate T_c involves the use of the nominal operating cell temperature (NOCT) [19], defined as a device temperature in the nominal terrestrial environment (NTE): solar irradiance of 800 W/m ^{2} (G_{NOCT}); T_a of 20 $^\circ$ C ($T_{\text{a,NOCT}}$); average V_w of 1 m/s ($V_{\text{w, NOCT}}$); zero electrical charge (open circuit); independent assembly structure oriented "normal to solar noon" [20], [21].

Standard conditions are employed to the PV module performance "classification" or "specification." The associated performance parameters are usually the manufacturer's nameplate ratings (specifications) or results of tests from a module testing laboratory. These performance specifications accuracy is fundamental to the design of PV plants, the reference point is provided from which performance in all other operating conditions is supplied [22]. Ideally, NOCT must be exactly the same regardless the testing laboratory, location, month or season [23]. In [24], a modification of the method for obtaining NOCT is proposed to calculate the called "realistic nominal module temperature," more representative in outdoor since in NOCT conditions, conditions of exposure are "open circuit," that do not count for the electrical energy withdrawal.

If not available from the data provided by the module manufacturer, the necessary parameters can be measured during outdoor tests under real operating conditions [25]. In BIPV plants, the modules are installed at an optimum distance from the building facade; as a result, the energy balance is not limited to the module layers. In this case, both sides of the modules are under quite different environmental conditions and the simple NOCT model can underestimate T_c by up to 20 K [26]. Consequently, in such applications a system of three equations simultaneously is needed, an energy balance for each of the three layers—PV module, the air layer between the module and the wall, and the wall—resulting in the respective equations, featuring each temperature. Such balances consider heat transfer among layers, ambient, and interior space. The methodology involves a lumped analysis approach, adopting uniform conditions along the gap; in more detailed studies are employed dynamic models and computational fluid dynamics (CFD) methods [27], [28].

From a mathematical viewpoint, the T_c models can be explicit, providing T_c directly, or implicit, involving variables that depend on T_c. In the second case, is required an interactive procedure [29]. Implicit models are based on the module's thermal properties and heat transfer mechanisms. T_c is interactively determined from an energy balance applied to the module. The explicit methods calculate T_c using known parameters [7]. T_c can be associated to the module back side temperature (T_b). The difference between both temperatures depends on the substrate materials of the module, and the G levels. A simple implicit empirical thermal model relating T_c and T_b has been successfully applied to several module arrangements, providing the expected T_c value with an accuracy of about $\pm$ 5 °C [see (1)]. This magnitude of T_c uncertainties result in an effect of less than 3% on the module power output [3]

TABLE I
ROSS PARAMETERS FOR VARIOUS INSTALLATIONS [33]

PV array mounting type	r (K m^2/W)
Free standing	0.021
Flat roof	0.026
Sloped roof well-cooled	0.020
Sloped roof not so well-cooled	0.034
Sloped roof highly integrated, poorly ventilated	0.056
Facade integrated transparent PV	0.046
Facade integrated opaque PV	0.054

$$T_c = T_b + \frac{G}{G_{\text{ref}}}\Delta T. \tag{1}$$

G is the solar irradiance on the PV module (W/m^2), G_{ref} = solar irradiance at standard test conditions (STC) (1000 W/m^2) and ΔT = temperature difference between T_c and T_b at G_{ref}.

The simplest explicit equation links T_c to the ambient temperature, T_a, and G [see (2)] [30]

$$T_c = T_a + rG. \tag{2}$$

This linear expression does not consider wind or electric charge, but a dimensional parameter r, the so-called Ross coefficient. Reported values for r vary and can be categorized qualitatively according to the level of integration and the space behind the modules [31], [32]. Some studies associate estimated values of r with different types of assembly arrangements/schemes [10] (see Table I).

Under NOCT conditions, (3) assumes the same T_a for both sides of the module, considering that the temperature difference (T_c - T_a) is practically independent of T_a, but linearly proportional to G [34]. Furthermore, the heat loss coefficient (U_L) is considered constant in this equation; this coefficient includes heat losses by convection, radiation, and conduction. Hence, the energy balance for an unitary area of the PV module is

$$T_c = T_a + \left(\frac{G}{G_{\text{NOCT}}}\right)\left(\frac{U_{\text{L,NOCT}}}{U_L}\right)(T_{\text{NOCT}} - T_{\text{a,NOCT}})\left[1 - \left(\frac{\eta}{\tau\alpha}\right)\right]. \tag{3}$$

In NOCT conditions, there is no-load operation, i.e., $\eta = 0$ [34]. Since η is a function of T_c, (3) is an implicit equation of T_c.

Values of cell's direct measurements include basic performance parameters (I_{sc} and maximum power point current, V_{oc} and maximum power point voltage) in the standard condition (reference), as well as other variables [35]. Methods based on the cell's direct measurements have proved to be more accurate than methods based on meteorological parameters for T_c estimation. The last presents more uncertainties associated to the sources of data and the model itself [18], but it is a very useful tool considering the advantage that T_c can be estimated at any location using meteorological data [36].

The use of a method based on the cell's direct measurements has the benefit of obtaining the parameters from the scientific literature or manufacturer data [37], [38]. However, precise parameter values are required because the given methods are highly sensitive to the chosen values. It is assumed that the spectral influence, module temperature coefficients, and optical losses are available in the results of tests with individual modules. This kind of mathematical model includes internal losses associated with wiring resistance and module incompatibility, values difficult to predict or explicitly determine. Other methods based on direct measurements have the disadvantage that the parameters should be adjusted by outdoor experimental tests—such as requiring a module with a cell temperature sensor for example—or from internal measurements in a sun simulator.

Considering a set of PV modules, the thermal model usually considers the modules as an unity. In general, the effect of incompatibility and resistance losses is small ($< 5\%$) in relation to the expected performance of the nameplate classifications of the individual modules [3]. Optimally, performance measurements are available at the arrangement level, improving the model accuracy. Once developed, the model can be applied for autonomous PV power plants; such plants are more complex than grid connected systems, since they can include batteries for energy storage and generators as auxiliary energy source.

The T_c correlations found in the literature from the year 2000 onward, are shown in Table II, including pertinent comments for the correlations. These equations have been developed considering a specific assembly geometry or a building integration level; hence, care should be taken when applying any of them. Depending on the specific application, some methods may be more suitable than others. Choose the most suitable method is not easy and depends mainly on the availability of module's data, the necessary precision and technical issues.

III. General Forms of the Correlations

Analyzing the equations of Table II, correlations 1–20 are linear and can be expressed by (4). ISFOC model (Correlation 21 in Table II) is linear if the terms in parentheses are assumed to be constant.

$$T_c = a_0 + a_1 T_a + a_2 G + a_3 V_w + a_4 T_b. \tag{4}$$

The terms a_0, a_1, a_2, a_3, and a_4 are specific for each of the mentioned linear models and are specified in Table V presented in the Appendix.

Correlations 22–30 of Table II are nonlinear and can be expressed by 5. Sandia's model can fit into this general expression if $\Delta T = (T_c - T_b) G_{ref}$ is constant

$$T_c = b_0 + b_1 T_a + C_1 (e^{d_1 + d_2 V_w} + e_1) G + C_2 (e_2 + f_1 T_a)^{g_1} (e_3 + f_2 G)^{g_2} (e_4 + f_3 V_w)^{g_3}. \tag{5}$$

The terms $b_0, b_1, C_1, d_1, d_2, e_1, C_2, e_2, f_1, g_1, e_3, f_2, g_2, e_4, f_3$, and g_3 are specific for each of the mentioned nonlinear models and are specified in Table VI presented in the Appendix. Kurtz *et al.* model is a particular case of the Hornung *et al.* model. Duffie and Beckman II and Mattei models are nonlinear and can be expressed in the form of (6).

$$T_c = (h_1 T_a + h_2 G)(m_1 + n_1 G)^{-1}. \tag{6}$$

The terms $h_1 0$, h_2, m_1, and n_1 are specific for Duffie and Beckman II and Mattei models and are specified in Table VII presented in the Appendix. Summarizing, all models of Table II can be grouped in the form of one of the equations defined above according to their terms.

IV. Main Models Parameters

The thermal properties of materials and environmental conditions have a great influence on T_c as part of the solar irradiation is converted into heat [68]. T_c depends heavily on G and T_a and is very sensitive to V_w [69], [70]. In this section, we highlight the parameters that have the greatest influence on T_c, considering the number of correlations. Considering the 33 correlations analyzed, G; T_a; V_w; η; solar absorption; glass cover transmittance are the most frequent (see Table III), appearing in: 100%, 93,9%, 54.5%, 33.3%, 30.3%, and 24.2% of the correlations, respectively. These parameters are grouped in meteorological variables and properties dependent on the material and/or system configuration.

A. Meteorological Variables

Generally, models for determining T_c use solar data dependent on the location, meteorological data obtained through recognized databases or meteorological models [71], [72]. Estimates of hourly averaged values are usually applied in thermal models to predict the associated T_c. If not, methods based on meteorological parameters require an outdoor experimental campaign to obtain G, T_a, and V_w values and parameters. Data estimate and/or average generates uncertainty related with the tabulated values and the thermal models. When using measurement instruments, models are also not free from uncertainties; there may be external influences or flaws in the measurement and accuracy of the instrument, depending on the experimental arrangement. Some technical difficulties are discussed, such as a system that blocks sunlight [73], the requirement of a solar simulator [74], the need for the entire module *I–V* curve [75] and the need for advanced knowledge in some specific issues.

1) Effective Irradiance: The output power of the PV cell is directly proportional to G incident on its surface [8]. Hence, measurements or estimates of G in a specific location are essential to predict the performance and efficiency of PV systems [76], [77]. G produces heat transfer by radiation, which is the most influential factor on T_c variations [78]. For an increase of 100 W/m ^{2} in G, increases in T_c between 1.8 °C and 4.93 °C are found in the literature, these values are not universal and depend on the type of PV module [55]. Some devices are specifically designed to measure G, as the irradiance meter and the pyranometer [79], [80]. In addition to these, cost-effective tools are found in the literature to estimate G [81]. Often the most important source of error in determining PV power is related with the procedure and instrument chosen to quantify G [3]. This is due to the different systematic influences on the test

TABLE II
EQUATIONS FOR T_C FROM THE YEAR 2000 ONWARDS INCLUDING PERTINENT COMMENTS

N°	Correlations name	Formulation	Comments	References
1	Fernández *et al.*[1]	$T_c = \frac{(V_{OC} - c_1 G - c_3)}{c_2}$	c_1, c_2 and c_3 are linear coefficients	[18], [16]
2	Durisch *et al.*	$T_c = T_a + kG$	$k = \frac{\Delta T_c}{\Delta G}$: 0.02 - 0.04°Cm²/W	[39], [40]
3	Nordmann and Clavadetscher	Same as above	$0.02 < k < 0.056$ for BIPV situations	[10], [32]
4	Krauter	Same as above	$k = 0.03, 0.012, 0.0058$ for conventional, upper or lower module in packaged home system, respectively	[41]
5	Mondol *et al.* I	$T_c = T_a + 0.031G$	For V_W above 1m/s with a constant heat loss coefficient	[10], [42], [43]
6	Hove	$T_c = T_a + G\left(\frac{\tau\alpha - \eta}{U_L}\right)$	$\frac{\tau\alpha}{U_L}$ determined experimentally	[10], [44]
7	Tiwari	$T_c = T_a + G\left(\frac{\tau\alpha}{U_L}\right)\left[1 - \left(\frac{\eta}{\tau\alpha}\right)\right]$	$\frac{\tau\alpha}{U_L}$ taken as constant	[10], [45]
8	Eicker	$T_c = T_a + G\left(\frac{\alpha}{U_L}\right)\left[1 - \frac{\eta}{\alpha}\right]$	U_L = h_{radn} + h_{conv}. Where h_{conv} and h_{radn} are coefficients of convection and radiation respectively	[10], [46]
9	Standard	$T_c = T_a + \left(\frac{G}{G_{NOCT}}\right)(T_{c,NOCT} - T_{a,NOCT})$	Steady state model for a flat plate module including crystalline silicon devices and thin-film cells	[7], [8], [4], [29], [47], [48], [49], [50], [51]
10	Davis	$T_c = T_a + \left(\frac{G}{G_{NOCT}}\right)(T_{c,NOCT} - T_{a,NOCT})\left[1 - \left(\frac{\eta}{\tau\alpha}\right)\right]$	Assumes U_L constant	[10], [26]
11	Mondol *et al.* II	$T_c = T_a + 0.031G - 0.058$	For V_W above 1m/s with a constant heat loss coefficient	[10], [6], [52]
12	Tselepis	$T_c = 30 + 0.0175(G - 150) + 1.14(T_a - 25)$	Estimates T_c for an a-Si module	[6], [53]
13	Tiwari and Sodha I	$T_c = \frac{pG(\tau\alpha - \eta) + (U_t T_a + U_T T_b)}{(U_t + U_T)}$	U_t, U_T: heat transfer coefficients specified in [54]	[55], [54], [56], [57]
14	Tiwari and Sodha II	$T_c = \frac{\tau[\alpha_C p + \alpha_\gamma (1 - \beta_c) G - \eta_c G \beta_c + U_t T_a + U_T T_b]}{(U_t + U_T)}$	T_b function of the product ηT_c	[10], [54]
15	Almonacid [1]	$T_c = T_a + d_1 G + d_2 V_W$	$d1, d2$: multilinear regression parameters	[18], [58]
16	Markvart	$T_c = 0.943 T_a + 4.3 + 0.028G - 1.528 V_W$		[6], [48], [59]
17	Muzathik	$T_c = 0.943 T_a + 0.3529 + 0.0195G - 1.528 V_W$		[6], [60]
18	Akyuz *et al.*	$T_c = 0.95 T_a + 3.1 + 0.025G - 0.3 V_W$		[6], [61]
19	NOCT-1p model	$T_c = T_a + \left(\frac{G}{G_{NOCT}}\right)(T_{c,NOCT} - T_{a,NOCT}) + a(V_W - V_{W,\,NOCT})$	a: parameter determined by data empirical fitting	[7]
20	NOCT-2p model	$T_c = T_a + b\left(\frac{G}{G_{NOCT}}\right)(T_{c,NOCT} - T_{a,NOCT}) + c(V_W - V_{W,\,NOCT})$	b and c: empirical parameters	[7]
21	ISFOC method[1]	$T_c = T_b + \left(\eta C_g \sum \frac{L_i}{\lambda_i}\right) G$	i, L_i and λ_i: layers, thickness and thermal conductivity of material behind the cell, respectively	[62]
22	Faiman	$T_c = T_a + \frac{G}{U_0 + U_1 V_W}$	U_0, U_1: specified in [24] for selected PV cells	[24], [29], [63]
23	Skoplaki and Palyvos	$T_c = T_a + \frac{0.32}{8.91 + 2V_W} G$	Estimates T_c for a p-Si module	[10], [6]
24	Skoplaki *et al.*I	$T_c = T_a + \frac{0.25}{5.7 + 3.8V_W} G$		[10], [6]
25	Duffie and Beckman I	$T_c = T_a + \frac{G(T_{c,NOCT} - T_{a,NOCT})}{G_{NOCT}}\left(\frac{9.5}{(5.7 + 3.8V_W)}\right)\left[1 - \left(\frac{\eta}{\tau\alpha}\right)\right]$	$\tau\alpha \approx 0.9$	[34]
26	Skoplaki *et al.* II	$T_c = T_a + \frac{G(T_{c,NOCT} - T_{a,ref})}{G_{NOCT}}\left[\frac{h_{NOCT}}{h}\left\{1 - \frac{\eta_{STC}}{\tau\alpha}(1 + \beta_{STC} T_{STC})\right\}\right]$	h = wind convection coefficient, h = 5.7 + 3.8Vw or h = 8.91 + 2.0Vw specified in [33]	[29], [33], [51]
27	Chenni *et al.*	$T_c = T_a + 0.0138G(1 + 0.031T_a)(1 - 0.042V_W)$	Estimates T_c for a Policristaline module	[10], [53], [59]
28	Kurtz *et al.*	$T_c = T_a + Ge^{-3.473 - 0.0594V_W}$	Estimates T_c for different PV technologies	[6], [51], [64]
29	Hornung *et al.*[1]	$T_c = T_a + m\left[e^{\left(\frac{-0.5V_W}{V_{W0}}\right)} + c\right] G$	m, V_{W0} and c: coefficients obtained by multilinear regression specified in [65]	[18], [65]
30	Coskun *et al.*	$T_c = 1.4T_a + 0.01(G - 500) - {V_W}^{0.8}$	Estimates T_c for a Policristaline module	[6]
31	Sandia's model	$T_c = T_b + \left(\frac{G}{G_{ref}}\right)\Delta T$ and $T_b = G\left(e^{a + b.V_W}\right) + T_a$	a and b: empirical parameters. $\Delta T = Tc - Tb$ at G_{ref} Adapted for High Concentrating Photovoltaic (HCPV) modules in [18]	[3], [10], [18]
32	Duffie and Beckman II	$T_c = \frac{T_a + \frac{G}{G_{NOCT}}(T_{c,NOCT} - T_{a,ref})\left\{1 - \frac{\eta_{STC}}{\tau\alpha}(1 + \beta_{STC} T_{STC})\right\}}{1 - \frac{\beta_{STC}\eta_{STC}}{\tau\alpha}\frac{G}{G_{ref,NTE}}(T_{c,NOCT} - T_{a,ref})}$		[29], [34], [66]
33	Mattei	$T_c = \frac{UT_a + G(\tau\alpha - \eta_{STC} - \beta_{STC}\eta_{STC} T_{STC})}{U - \beta_{STC}\eta_{STC} G}$	U: heat exchange coefficient for the module surface. U = 26.6 + 2.3v or U = 24.1 + 2.9v, specified in [67]. $\tau\alpha = 0.81$	[7], [10], [29], [51], [67]

[1] Applied to HCPV.

TABLE III
PARAMETERS OF THE ANALYZED EQUATIONS (✓ MEANS A PARAMETER OF THE CORRELATION, × OTHERWISE)

Correlations vs parameters	G	T_a	V_w	η	α	τ	G_{NOCT}	$T_{c,NOCT}$	$T_{a,NOCT}$	β	U	Other inputs (appear in five or less of the studied correlations)
Fernández *et al.*	✓	×	✓	×	×	×	×	×	×	×	×	V_{oc}, c_1, c_2, c_3
Durisch *et al.*	✓	✓	×	×	×	×	×	×	×	×	×	k
Nordmann and Clavadetscher	✓	✓	×	×	×	×	×	×	×	×	×	k
Krauter	✓	✓	×	×	×	×	×	×	×	×	×	k
Mondol *et al.* I	✓	✓	×	×	×	×	×	×	×	×	×	
Hove	✓	✓	×	✓	✓	✓	×	×	×	×	✓	
Tiwari	✓	✓	×	✓	✓	✓	×	×	×	×	✓	
Eicker	✓	✓	×	✓	✓	×	×	×	×	×	✓	
Standard	✓	✓	×	×	×	×	✓	✓	✓	×	×	
Davis	✓	✓	×	✓	✓	✓	✓	✓	✓	×	×	
Mondol *et al.* II	✓	✓	×	×	×	×	×	×	×	×	×	
Tselepis	✓	✓	×	×	×	×	×	×	×	×	×	
Tiwari and Sodha I	✓	✓	×	✓	✓	✓	×	×	×	×	×	p, T_b, U_t,U_T
Tiwari and Sodha II	✓	✓	×	✓	✓	✓	×	×	×	✓	×	p, T_b, U_t, U_T
Almonacid	✓	✓	✓	×	×	×	×	×	×	×	×	d_1,d_2
Markvart	✓	✓	✓	×	×	×	×	×	×	×	×	
Muzathik	✓	✓	✓	×	×	×	×	×	×	×	×	
Akyuz *et al.*	✓	✓	✓	×	×	×	×	×	×	×	×	
NOCT-1p model	✓	✓	✓	×	×	×	✓	✓	✓	×	×	a,$V_{w,\text{ NOCT}}$
NOCT-2p model	✓	✓	✓	×	×	×	✓	✓	✓	×	×	b, c, $V_{w,\text{ NOCT}}$
ISFOC method	✓	×	×	✓	×	×	×	×	×	×	×	T_b, C_g, L_i, λ_i
Faiman	✓	✓	✓	×	×	×	×	×	×	×	×	U_0, U_1
Skoplaki and Palyvos	✓	✓	✓	×	×	×	×	×	×	×	×	
Skoplaki *et al.* I	✓	✓	✓	×	×	×	×	×	×	×	×	
Duffie and Beckman I	✓	✓	✓	✓	✓	✓	✓	✓	✓	×	×	
Skoplaki *et al.* II	✓	✓	✓	✓	✓	✓	✓	✓	✓	✓	×	h, h_{NOCT}, T_{STC}
Chenni *et al.*	✓	✓	✓	×	×	×	×	×	×	×	×	
Sandia's model	✓	✓	✓	×	×	×	×	×	×	×	×	G_{ref}, e, a, b
Kurtz *et al.*	✓	✓	✓	×	×	×	×	×	×	×	×	
Hornung *et al.*	✓	✓	✓	×	×	×	×	×	×	×	×	m, V_{w0}, c
Coskun *et al.*	✓	✓	✓	×	×	×	×	×	×	×	×	
Duffie and Beckman II	✓	✓	×	✓	✓	×	✓	✓	✓	✓	×	T_{STC}
Mattei	✓	✓	✓	✓	✓	✓	×	×	×	✓	✓	T_{STC}

TABLE IV
ISC-VOC METHODS FOR T_c INCLUDING PERTINENT COMMENTS

Correlations name	Formulation	Coments	References
Muller[1]	$T_c = T_{h,0} + \frac{(V_{max} - V_{oc(t)})}{(N_s \beta)}$	$\beta = -0.0045$ (V/C/cell). N_s: Number of cells in series in a module. $T_{h,0}$:Heat sink temperature at shutter initiation specified in [73]	[18], [73]
Voc–Isc method[1]	$T_c = \frac{V_{oc} - V_{ocr} + \beta(C_g)T_r}{\frac{nk}{q} ln \frac{I_{sc}}{I_{scr}} + \beta(C_g)}$	$T_r = 298.15$ Kelvin Reference temperature	[3], [73], [104]
Improved Voc–Isc method	$T_c = \frac{V_{oc} - V_{ocr} - \frac{nkT_r}{q} ln(C_g)}{\frac{nk}{q} ln(C_g) + \beta} + T_r$	Similar to the model presented by [3] for $C_g = 1$	[3], [73], [104]
IEC 60904-5 method	$T_c = \frac{\beta T_{c,ref} + V_{oc} - V_{ocr} + \frac{nk}{q} ln\left(\frac{G_{ref}}{G}\right) 273 N_s}{\beta - \frac{nk}{q} ln\left(\frac{G_{ref}}{G}\right) N_s}$	$T_{c,ref}$ is the T_c at the STC conditions	[37]

results: the response of the module and the G sensor may vary; the orientation and the optical acceptance angle or the module and the G sensor viewing angle may differ, the response of the module and the G sensor varies significantly depending on the incidence angle [82]. In addition, in case of shading or dust, the value detected by the measuring instrument and the G value on the cell can be different [83], [84].

The concept of "effective G" provides a method for reduce the difficulty and uncertainty related with PV plants field testing and for dealing with the mentioned systematic influences. The effective G is the G on the module plane to which the PV cells really respond, upon the optical losses influences and solar spectral variation due to the angle of solar incidence and the module dirtiness. Depending on the required precision and the available measured data, different approaches can be used to determinate the effective G as demonstrated in [81], where the authors propose a smartphone-aided accessible setup to estimate the solar irradiance in a certain location. And in [82], where the authors measure irradiance using a mobile multipyranometer array with five pyranometers.

2) Wind Speed: The V_{w} value becomes a relevant environmental variable, favoring heat loss by convection. The results of the sensitivity analysis for a polycrystalline PV module type 125G-2 are reported in [47]: a T_{c} drop of 3.3 °C is quantified when V_{w} increases from 1 to 2 m/s; this value is not universal and depend on the type of PV module and type of materials used. Monitoring and/or establishing uniform conditions for relevant wind measurements, especially in field, is not a simple task. Hence, many correlations using heat transfer coefficients related to V_{w} can be found in the scientific literature in recent years [85].

The low availability of local data is a barrier to ensure accurate results for assessing the real efficiency of operation in situations, where T_{c} plays a fundamental role [86]. Consequently, some of the PV system efficiency simulators that base T_{c} on environmental variables usually disregard V_{w}. An option to replace field measurements is local data from numerical climate prediction models [51], [87].

The standard meteorological practice for V_{w} and wind direction record, locates the measurement device, anemometer, at the height of 10 m in an area with a minimum number of structures or buildings that could obstruct air movement [3]. However, in some studies, after installing the system, the thermal model can be "adjusted" by determining coefficients that compensate for location-dependent influences and installations of anemometers that are different from standard meteorological practice [88].

The empirically determined coefficients also vary for different types of modules and mounting configurations [89]. In some cases, a generic coefficient is presented for typical flat plate PV modules from distinct manufacturers. Nevertheless, the thermal behavior of the concentrator modules can vary significantly, depending on the module design [73], [74]. Therefore, concentrator coefficients must be determined empirically for each module project.

The wind direction can have a small but noticeable influence on T_{c}. However, the incorporation of the wind direction effect in the thermal model is unnecessarily complex [51]. Therefore, in most studies, the influence of the wind direction on T_{c} is disregarded or considered as a random influence, adding uncertainty to the thermal model.

3) Ambient Temperature: The T_{a} value has proved to be an important variable in models, influencing η and T_{c} [90]. For a polycrystalline PV module T_{c} increases around 1 °C when T_{a} gains 1 °C, this increase depends on the type of PV module [47]. Almost all T_{c} models require T_{a} as input. Monitoring T_{a} does not present a major challenge, considering the high precision devices available in the market, with a considerable operating range and resolution at an acceptable cost. Moreover, T_{a} accurate monitoring techniques are already known and established [91]. Globally, the scientific literature have shown that the PV performance rate increases with the altitude due to the low temperature. Regions with high altitude such as the southern Andes, the region of Himalayan and Antarctica have demonstrated the largest PV potentials [92].

B. Properties Dependent on the Material and System Configuration

1) PV Cell/Module Electrical Efficiency: The η value decays with increasing T_{c} [93]. For crystalline PV modules under an irradiance of 1000 W/m ^{2}, η decreases around 0.03–0.06% with 1 °C increase in T_{c} [55]. Hence, η is a a parameter present in a large number of correlations and depends on the PV cell electrical parameters such as V_{oc}, FF, and I_{sc}, and G [93]. Usually, the manufacturer provides the values of η, V_{oc}, I_{sc}, and FF under standard conditions, since these parameters are directly linked to the production of the cell/module. These variables can be obtained experimentally [94], each of them providing information about the device physics [95].

2) Solar Absorption and Transmittance of PV Module Glass Cover: The solar energy incident on a body can be absorbed, reflected, and/or passed through the material. This characteristic can be seen in all semitransparent materials, represented by the well-known coefficients of transmissivity (τ), reflectivity, and absorbance (α) [96]. These coefficients are dependent on G and influence the rate of irradiance converted by the PV cell [9]. Usually, cells are manufactured to maximize the absorption of the wavelengths [97]. The radiation energy absorbed by the glass cover is represented by (7)

$$Q_{\mathrm{g}} = G\alpha = G(1 - \tau_A). \tag{7}$$

τ_A is the glass transmittance considering loss only through absorption [98].

The α value appears in correlations of T_{c} both independently and through the product $\tau\alpha$ [99]. Mathematical models relating the sensitivity of the manufacturing parameters to the electrical and thermal efficiency of PV devices have shown that there are gains when considering the product $\tau\alpha$ [97]. The influence of optical losses (reflectance) for flat plate modules is usually negligible to G incidence angles under 55 °. Such losses for a not oriented perpendicular to the sunlight path module surface are added to the typical "cosine" loss. Hence, the cumulative effect (loss) over the year must be considered in system design. For modules that accurately track the sun, there is no optical loss [3].

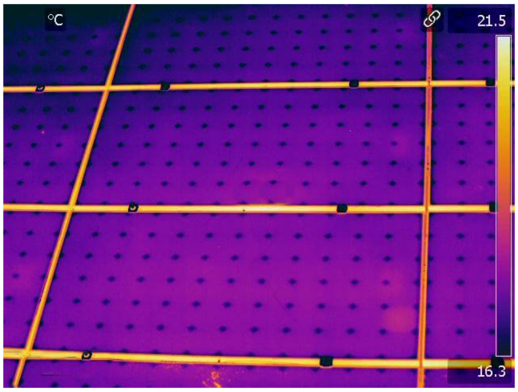

Fig. 2. PV module infrared thermal image. Adapted from [103].

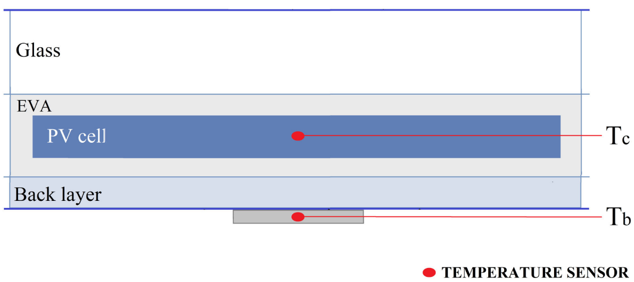

Fig. 3. Representation of the PV cell showing ideal measurement position of T_c.

3) Other Factors: Various coefficients appear in the literature that are related to T_c, influenced by the module construction, the assembly configuration and the location and height at which V_w is measured. There are also the so-called factors that "introduce random influences" in T_c, such as the module thermal capacitance and thermal transients caused by clouds, shading, humidity, and dust [100], [101]. These random effects are averaged daily or annually.

V. Validation of Models by T_c Determination

The cells operate at slightly different temperatures throughout a PV module [63]. To register such behavior, thermography allows reliable monitoring of the PV plant temperature [102], according to Fig. 2. Considering this temperature difference, researchers mention an "average cell temperature," or just "cell temperature," T_c [18]. PV cell is surrounded by encapsulating materials; hence, a direct measurement of T_c true value is not possible in general. The concept of T_c is not usually clearly defined, depending on the methodology and technique used.

The measurement of T_c true value can be implemented inside the PV module structure, between PV cell and the ethylene vinyl acetate (EVA) coating [105] (see Fig. 3). T_c can be obtained empirically, a nontrivial work, or estimated through a mathematical relationship with T_b, based on the 1-D thermal conduction through the module materials. T_c is then calculated using T_b and a difference between the cell and the back-surface temperature.

In most cases, authors consider the module temperature as the temperature of a representative cell or the mean value of several cells. This temperature can be measured by a sensor attached on the module back-surface, the measured value is the module temperature. Measuring the temperature by a sensor fixed on the back of the PV module is common practice to estimate T_c [7]. Generally, the PV module temperature is measured by connecting several temperature sensors (thermocouples) attached to the module back side; however, in the reality, the sensors detect the lower layer temperature. T_c can be higher than T_b by a few degrees, this difference depends on the module substrate materials and G. For flat modules in an open arrangement, T_c is less sensitive to V_w than T_b, as the cell is inside the module structure, while the back-surface is directly exposed to the wind [105]. For flat modules in which the back-surface is thermally insulated, it can be assumed zero temperature difference between T_c and T_b.

The influence of V_w, wind direction, structural support components, junction boxes, and module structures may cause nonuniform temperature distributions across the module surface. Typically, these spatial temperature differences vary by about 5 °C. The module central cells have higher temperatures than those close to the module edges [47]. So, a careful placement of the thermocouples helps to obtain a accurate value for the average module temperature. The spatial temperature variation in the module can be compensated by the average of several temperature measurements, resulting in a reliable average of T_b.

Methods based on electrical parameters consider that V_{oc} vary with temperature. Isc–Voc methods can be used for extracting T_c from *I–V* curve measurements and the results are useful for T_c validation. These methods are not used to "model" T_c from weather, they are expressed as a function of the electrical parameters of the PV cell/module, and can be classified as a different class of nonlinear models. It is not possible to compare the functional form of the Isc–Voc methods with Table II models, as the parameters are different. Some Isc–Voc methods are represented in Table IV.

The T_c value can also be estimated based on environmental parameters. However, this estimate has uncertainties that affect the precision of the performance model [3]. Other methods require an outdoor experimental campaign with a module with an internal cell temperature sensor. This type of device is not always available and the procedure takes time to perform measurements. Studies comparing the temperature measured with an internal sensor inserted just below the cell, with the temperature obtained using models based on the heat flow calculation using T_b, show an accuracy of ± 1 °C [105]. Hence, the application of models that associate T_b to T_c has shown to be attractive since T_b can be easily obtained, while the temperature measurement using a PV module with an internal sensor, although accurate, is difficult and expensive [18]. However, it should be considered that for a reliable design and a performance estimate of PV plants, accurate and easy to implement models are needed [9].

VI. Conclusion

The T_c value is a critical parameter to characterize PV modules behavior. In order to help researchers and professionals to choose the significant variables and the most appropriate experimental arrangements to compose an accurate prediction model, we review relevant contributions of PV modules operating temperature models developed from the year 2000 onward. Strategies of obtaining T_c for model validation are also presented.

According to our study, correlations for T_c found in the literature apply to free-standing PV arrays, PV/thermal collectors and BIPV installations. These correlations express T_c as a function of meteorological variables and include material and system dependent properties as parameters. Most of the models for the determination of T_c can be conveniently represented according to their parameters by one of the three in this article proposed general forms: one linear and two nonlinear. As a possible application, the proposed general forms can help the development of algorithms for continuous and automatic adjustment of models over time, based on machine learning.

The variables with the greatest influence, appearing in a significant number of models, are: solar absorption, η, transmittance, G, T_a, and V_w. Solar absorption appears in correlations independently or in the product $\tau\alpha$. The manufacturer usually provides the η value; if not, the parameter can be obtained empirically using some techniques. Often the most significant source of errors in determining PV power is associated with the procedure and instrument applied to quantify G. Therefore, attention should be paid to determining the "effective G." Installations of anemometers different from standard meteorological practice, for different types of modules and mounting configurations, require adjustment through modeling. The influence of wind direction on T_c can be disregarded or considered to be a random influence.

The T_c value can be measured directly with an internal temperature sensor, obtained through correlation with T_b or estimated by models based on environmental parameters. The best strategy to obtain T_b for T_c estimation is connecting several temperature sensors and averaging the measurements. Hence, special attention should be taken when applying a generic expression to obtain T_c. Depending on the specific application, some methods may be more suitable than others.

APPENDIX

See Tables V–VII.

TABLE V
TERMS OF THE LINEAR CORRELATIONS WHEN EXPRESSED BY (4)

Correlations name	Formulation	a_0	a_1	a_2	a_3	a_4
Fernández *et al.*	$T_c = \frac{(V_{oc} - c_1 G - c_3)}{c_2}$	$\frac{(V_{oc} - c_3)}{c_2}$	0	$\frac{-c_1}{c_2}$	0	0
Durisch *et al.*	$T_c = T_a + kG$	0	1	k	0	0
Nordmann and Clavadetscher	Same as above	0	1	k	0	0
Krauter	Same as above	0	1	k	0	0
Mondol *et al.* I	$T_c = T_a + 0.031G$	0	1	0.031	0	0
Hove	$T_c = T_a + G\left(\frac{\tau\alpha - \eta}{U_L}\right)$	0	1	$\frac{\tau\alpha-\eta}{U_L}$	0	0
Tiwari	$T_c = T_a + G\left(\frac{\tau\alpha}{U_L}\right)\left[1 - \left(\frac{\eta}{\tau\alpha}\right)\right]$	0	1	$\left(\frac{\tau\alpha}{U_L}\right)\left[1 - \left(\frac{\eta}{\tau\alpha}\right)\right]$	0	0
Eicker	$T_c = T_a + G\left(\frac{\alpha}{U_L}\right)\left[1 - \frac{\eta}{\alpha}\right]$	0	1	$\left(\frac{\alpha}{U_L}\right)\left[1 - \frac{\eta}{\alpha}\right]$	0	0
Standard	$T_c = T_a + \left(\frac{G}{G_{NOCT}}\right)(T_{c,NOCT} - T_{a,NOCT})$	0	1	$\frac{(T_{c,NOCT}-T_{a,NOCT})}{G_{NOCT}}$	0	0
Davis	$T_c = T_a + \left(\frac{G}{G_{NOCT}}\right)(T_{c,NOCT} - T_{a,NOCT})\left[1 - \left(\frac{\eta}{\tau\alpha}\right)\right]$	0	1	$\left(\frac{T_{c,NOCT}-T_{a,NOCT}}{G_{NOCT}}\right)\left[1 - \left(\frac{\eta}{\tau\alpha}\right)\right]$	0	0
Mondol *et al.* II	$T_c = T_a + 0.031G - 0.058$	−0.058	1	0.031	0	0
Tselepis	$T_c = 30 + 0.0175(G - 150) + 1.14(T_a - 25)$	$[30 - 0.0175(150) - 1.14(25)]$	$1.14T_a$	$0.0175G$	0	0
Tiwari and Sodha I	$T_c = \frac{pG(\tau\alpha-\eta)+(U_t T_a + U_T T_b)}{(U_t+U_T)}$	0	$\frac{U_t}{(U_t+U_T)}$	$\frac{p(\tau\alpha-\eta)}{(U_t+U_T)}$	0	$\frac{U_T}{(U_t+U_T)}$
Tiwari and Sodha II	$T_c = \frac{\tau[\alpha_C p + \alpha_\gamma(1-\beta_c)G - \eta_c G \beta_c + U_t T_a + U_T T_b]}{(U_t+U_T)}$	$\frac{\tau\alpha_C p}{(U_t+U_T)}$	$\frac{\tau U_t}{(U_t+U_T)}$	$\frac{\tau\alpha_\gamma(1-\beta_c-\eta_c\beta_c)}{(U_t+U_T)}$	0	$\frac{\tau U_T}{(U_t+U_T)}$
Almonacid	$T_c = T_a + d_1 G + d_2 V_w$	0	1	d_1	d_2	0
Markvart	$T_c = 0.943T_a + 4.3 + 0.028G - 1.528V_w$	4.3	0.943	0.028	−1.528	0
Muzathik	$T_c = 0.943T_a + 0.3529 + 0.0195G - 1.528V_w$	0.3529	0.943	0.0195	−1.528	0
Akyuz *et al.*	$T_c = 0.95T_a + 3.1 + 0.025G - 0.3V_w$	3.1	0.95	0.025	−0.3	0
NOCT-1p model	$T_c = T_a + \left(\frac{G}{G_{NOCT}}\right)(T_{c,NOCT} - T_{a,NOCT}) + a(V_w - V_{w,\,NOCT})$	$-aV_{w,\,NOCT}$	1	$\left(\frac{T_{c,NOCT}-T_{a,NOCT}}{G_{NOCT}}\right)$	a	0
NOCT-2p model	$T_c = T_a + b\left(\frac{G}{G_{NOCT}}\right)(T_{c,NOCT} - T_{a,NOCT}) + c(V_w - V_{w,\,NOCT})$	$-cV_{w,\,NOCT}$	1	$b\left(\frac{T_{c,NOCT}-T_{a,NOCT}}{G_{NOCT}}\right)$	c	0
ISFOC method	$T_c = T_b + \left(\eta C_g \sum \frac{L_i}{\lambda_i}\right) G$	0	0	$\left(\eta C_g \sum \frac{L_i}{\lambda_i}\right)$	0	1

TABLE VI
TERMS OF THE NONLINEAR CORRELATIONS WHEN EXPRESSED BY (5)

Correlations name	Formulation	b_0	b_1	C_1	d_1	d_2	e_1	C_2	e_2	f_1	g_1	e_3	f_2	g_2	e_4	f_3	g_3
Faiman	$T_c = T_a + \frac{G}{U_0 + U_1 V_w}$	0	1	0	-	-	-	1	1	0	1	0	1	1	U_0	U_1	−1
Skoplaki and Palyvos	$T_c = T_a + \frac{0.32}{8.91 + 2V_w}G$	0	1	0	-	-	-	1	1	0	1	0	0.32	1	8.91	2	−1
Skoplaki *et al.*I	$T_c = T_a + \frac{0.25}{5.7 + 3.8V_w}G$	0	1	0	-	-	-	1	1	0	1	0	0.25	1	5.7	3.8	−1
Duffie and Beckman I	$T_c = T_a + \left(\frac{G}{G_{NOCT}}\right)\left(\frac{9.5}{(5.7+3.8V_w)}\right)(T_{c,NOCT} - T_{a,NOCT})\left[1 - \left(\frac{\eta}{\tau\alpha}\right)\right]$	0	1	0	-	-	-	1	1	0	1	0	$\frac{9.5(T_{c,NOCT}-T_{a,NOCT})}{\tau\alpha G_{NOCT}(\tau\alpha-\eta)^{-1}}$	1	5.7	3.8	−1
Skoplaki *et al.* II	$T_c = T_a + \frac{G}{G_{NOCT}}(T_{c,NOCT} - T_{a,ref})\left[\frac{h_{NOCT}}{h}\left\{1 - \frac{\eta_{STC}}{\tau\alpha}(1 + \beta_{STC} T_{STC})\right\}\right]$	0	1	0	-	-	-	1	1	0	1	0	$\frac{h_{NOCT}(T_{c,NOCT}-T_{a,ref})(\tau\alpha)^{-1}}{G_{NOCT}[\tau\alpha-\eta_{STC}(1+\beta_{STC}T_{STC})]^{-1}}$	1	a	b	−1
Chenni *et al.*	$T_c = T_a + 0.0138G(1 + 0.031T_a)(1 - 0.042V_w)$	0	1	0	-	-	-	0.0138	1	0.031	1	0	1	1	1	−0.042	1
Sandia's model	$T_c = T_b + \left(\frac{G}{G_{ref}}\right)\Delta T$ and $T_b = G\left(e^{a+b.V_w}\right) + T_a$	0	1	$\frac{\Delta T}{G_{ref}}$	a	b	0	0	-	-	-	-	-	-	-	-	-
Kurtz *et al.*	$T_c = T_a + Ge^{-3.473-0.0594V_w}$	0	1	1	−3.473	−0.0594	0	0	-	-	-	-	-	-	-	-	-
Hornung *et al.*	$T_c = T_a + m\left[e^{\left(\frac{-0.5V_w}{V_{w0}}\right)} + c\right]G$	0	1	m	0	$\frac{-0.5}{V_{w0}}$	c	0	-	-	-	-	-	-	-	-	-
Coskun *et al.*	$T_c = 1.4T_a + 0.01(G - 500) - V_w^{0.8}$	−0.01× 500	1.4	0.01	0	0	0	−1	1	0	1	1	0	1	0	1	0.8

If $C_1 = 0$, the terms d_1, d_2, and e_1 that depend on C_1 are disregarded and represented by "-." The same occurs with the terms e_2, f_1, g_1, e_3, f_2, g_2, e_4, f_3, and g_3 when $C_2 = 0$.

TABLE VII
TERMS OF THE NONLINEAR CORRELATIONS 32 AND 33 WHEN EXPRESSED BY (6)

Correlations name	Formulation	h_1	h_2	m_1	n_1
Duffie and Beckman II	$T_{\mathrm{c}} = \frac{T_{\mathrm{a}} + \frac{G}{G_{\mathrm{NOCT}}}(T_{\mathrm{c,NOCT}} - T_{\mathrm{a,ref}})\left\{1 - \frac{\eta_{\mathrm{STC}}}{\tau\alpha}(1 + \beta_{\mathrm{STC}} T_{\mathrm{STC}})\right\}}{1 - \frac{\beta_{\mathrm{STC}}\eta_{\mathrm{STC}}}{\tau\alpha}\frac{G}{G_{\mathrm{ref,NTE}}}(T_{\mathrm{c,NOCT}} - T_{\mathrm{a,ref}})}$	1	$\frac{(T_{\mathrm{c,NOCT}} - T_{\mathrm{a,ref}})}{G_{\mathrm{NOCT}}}\left\{1 - \frac{\eta_{\mathrm{STC}}}{\tau\alpha}(1 + \beta_{\mathrm{STC}} T_{\mathrm{STC}})\right\}$	1	$-\frac{\beta_{\mathrm{STC}}\eta_{\mathrm{STC}}}{\tau\alpha}\frac{(T_{\mathrm{c,NOCT}} - T_{\mathrm{a,ref}})}{G_{\mathrm{ref,NTE}}}$
Mattei	$T_{\mathrm{c}} = \frac{UT_{\mathrm{a}} + G(\tau\alpha - \eta_{\mathrm{STC}} - \beta_{\mathrm{STC}}\eta_{\mathrm{STC}} T_{\mathrm{STC}})}{U - \beta_{\mathrm{STC}}\eta_{\mathrm{STC}} G}$	U	$(\tau\alpha - \eta_{\mathrm{STC}} - \beta_{\mathrm{STC}}\eta_{\mathrm{STC}} T_{\mathrm{STC}})$	U	$-\beta_{\mathrm{STC}}\eta_{\mathrm{STC}}$

ACKNOWLEDGMENT

Leticia de Oliveira Santos would like to thank "Coordenação de Aperfeiçoamento de Pessoal de Nível Superior (CAPES)" for a M.Sc. scholarship. Paulo Cesar Marques de Carvalho would like to thank "Conselho Nacional de Desenvolvimento Científico e Tecnológico (CNPq)" for a researcher scholarship.

REFERENCES

[1] P. Trinuruk, C. Sorapipatana, and D. Chenvidhya, "Estimating operating cell temperature of BIPV modules in Thailand," *Renewable Energy*, vol. 34, no. 11, pp. 2515–2523, 2009.

[2] L. Gigoni *et al.*, "Day-ahead hourly forecasting of power generation from photovoltaic plants," *IEEE Trans. Sustain. Energy*, vol. 9, no. 2, pp. 831–842, Apr. 2018.

[3] D. L. King, J. A. Kratochvil, and W. E. Boyson, "Photovoltaic array performance model," Sandia Nat. Lab., Livermore, CA, USA, Rep. SAND2004-3535, Dec. 2004, doi: 10.2172/919131.

[4] A. Q. Jakhrani, A. Othman, A. R. H. Rigit, and S. R. Samo, "Determination and comparison of different photovoltaic module temperature models for kuching, sarawak," in *Proc. IEEE Conf. Clean Energy Technol.*, 2011, pp. 231–236.

[5] A. Shafieian, M. Khiadani, and A. Nosrati, "Theoretical modelling approaches of heat pipe solar collectors in solar systems: A comprehensive review," *Sol. Energy*, vol. 193, pp. 227–243, 2019.

[6] C. Coskun, U. Toygar, O. Sarpdag, and Z. Oktay, "Sensitivity analysis of implicit correlations for photovoltaic module temperature: A review," *J. Cleaner Prod.*, vol. 164, pp. 1474–1485, 2017.

[7] S. P. Mora, J. Carretero, and M. S.-de Cardona, "Models to predict the operating temperature of different photovoltaic modules in outdoor conditions," *Prog. Photovolt. Res. Appl.*, vol. 23, no. 10, pp. 1267–1282, 2015.

[8] S. P. Mora, M. Piliougine, J. Carretero, G. Nofuentes, and M. S.-de Cardona, "Empirical model to predict the operating temperature of the modules of a photovoltaic system," *Int. J. Smart Grid Clean Energy*, vol. 6, no. 1, pp. 40–46, Jan. 2017, doi: 10.12720/sgce.6.1.40-46.

[9] E. Cuce, P. M. Cuce, I. H. Karakas, and T. Bali, "An accurate model for photovoltaic (PV) modules to determine electrical characteristics and thermodynamic performance parameters," *Energy Convers. Manag.*, vol. 146, pp. 205–216, 2017.

[10] E. P. J. A. Skoplaki and J. A. Palyvos, "Operating temperature of photovoltaic modules: A survey of pertinent correlations," *Renewable Energy*, vol. 34, no. 1, pp. 23–29, 2009.

[11] G. Sala, "Cooling of solar cells," in *Solor Cells Optics Photovoltaic Concentration*, A. Luque, Ed. Philadelphia, PA, USA: A. Hilger, 1989, ch. 8, pp. 239–267.

[12] M. C. A. García and J. L. Balenzategui, "Estimation of photovoltaic module yearly temperature and performance based on nominal operation cell temperature calculations," *Renewable Energy*, vol. 29, no. 12, pp. 1997–2010, 2004.

[13] B. Marion, B. Kroposki, K. Emery, J. D.Cueto, D. Myers, and C. Osterwald, "Validation of a photovoltaic module energy ratings procedure at NREL," Nat. Renewable Energy Lab., Golden, CO, USA, Tech. Rep. NREL/TP-520-26909, 1999, doi: 10.2172/12187.

[14] T. Denoix, M. Sechilariu, and F. Locment, "Experimental comparison of photovoltaic panel operating cell temperature models," in *Proc. IEEE 40th Annu. Conf. Ind. Electron. Soc.*, 2014, pp. 2089–2095.

[15] S. Dubey, J. N. Sarvaiya, and B. Seshadri, "Temperature dependent photovoltaic (PV) efficiency and its effect on PV production in the world-a review," *Energy Procedia*, vol. 33, pp. 311–321, 2013.

[16] E. F. Fernández, G. Siefer, F. Almonacid, A. J. G. Loureiro, and P. Pérez-Higueras, "A two subcell equivalent solar cell model for III-V triple junction solar cells under spectrum and temperature variations," *Sol. Energy*, vol. 92, pp. 221–229, 2013.

[17] G. Siefer and A. W. Bett, "Analysis of temperature coefficients for III-V multi-junction concentrator cells," *Prog. Photovolt. Res. Appl.*, vol. 22, no. 5, pp. 515–524, 2014.

[18] P. Rodrigo, E. F. Fernández, F. Almonacid, and P. J. Pérez-Higueras, "Review of methods for the calculation of cell temperature in high concentration photovoltaic modules for electrical characterization," *Renewable Sustain. Energy Rev.*, vol. 38, pp. 478–488, 2014.

[19] L. Castañer, S. Bermejo, T. Markvart, and K. Fragaki, "IIIa-1 - Energy production by a PV array," in *Practical Handbook of Photovoltaics*, New York, NY, USA: Elsevier, 2003, pp. 517–529.

[20] J. W. Stultz and L. C. Wen, "Thermal performance testing and analysis of photovoltaic modules in natural sunlight," Jet Propulsion Lab., Pasadena, CA, USA, Report 5101-31, Jul. 1977, p. 31.

[21] ASTM E1036M-96e2, "Method for determining the nominal operating temperature (NOCT) of an array or module," Annex A.1. p.544. in: Standard Test Methods for Electrical Performance of Nonconcentrator Terrestrial Photovoltaic Modules and Arrays Using Reference Cells (Withdrawn 2005), ASTM Int., West Conshohocken, PA, USA, ASTM 684E1036M-96e2, 1996, doi: 10.1520/E1036M-96E02.

[22] R. N. Dows and E. J. Gough, "PVUSA procurement, acceptance, and rating practices for photovoltaic power plants," Pacific Gas Electric Co., San Ramon, CA, USA, Tech. Rep. DOE/AL/82993-21, 1995, doi: 10.2172/119944.

[23] J. Kuitche *et al.*, "One year NOCT round-robin testing per IEC 61215 standard," in *Proc. 37th IEEE Photovolt. Specialists Conf.*, 2011, pp. 2380–2385.

[24] M. Koehl, M. Heck, S. Wiesmeier, and J. Wirth, "Modeling of the nominal operating cell temperature based on outdoor weathering," *Sol. Energy Mater. Sol. Cells*, vol. 95, no. 7, pp. 1638–1646, 2011.

[25] D. L. King, J. A. Kratochvil, and W. E. Boyson, "Temperature coefficients for PV modules and arrays: Measurement methods, difficulties, and results," in *Proc. Conf. Rec. 26th IEEE Photovolt. Specialists Conf.*, 1997, pp. 1183–1186.

[26] M. W. Davis, A. H. Fanney, and B. P. Dougherty, "Prediction of building integrated photovoltaic cell temperatures," *J. Sol. Energy Eng.*, vol. 123, no. 3, pp. 200–210, 2001.

[27] R. Zhang, P. A. Mirzaei, and J. Carmeliet, "Prediction of the surface temperature of building-integrated photovoltaics: Development of a high accuracy correlation using computational fluid dynamics," *Sol. Energy*, vol. 147, pp. 151–163, 2017.

[28] P. A. Mirzaei and R. Zhang, "Validation of a climatic CFD model to predict the surface temperature of building integrated photovoltaics," in *Proc. Energy Procedia 6th Int. Building Phys. Conf.*, 2015, pp. 1865–1870. [Online]. Available: https://www.sciencedirect.com/science/article/pii/S1876610215020809

[29] H. Mohammed, R. Gupta, O. Sastry, and D. Magare, "Assessment of different correlations to estimate distinct technology PV module operating temperature for indian site," *Energy Sci. Eng.*, vol. 7, no. 3, pp. 1032–1041, 2019.

[30] R. G. Ross, "Interface design considerations for terrestrial solar cell modules," in *Proc. 12th IEEE Photovolt. Spec. Conf.*, 1976, pp. 801–806. [Online]. Available: https://ui.adsabs.harvard.edu/abs/1976pvsp.conf.801R

[31] M. Buresh, *Photovoltaic Energy Systems*. New York, NY, USA: McGraw-Hill Book Co, 1983, pp. 509–510.

[32] T. Nordmann and L. Clavadetscher, "Understanding temperature effects on FV system performance," in *Proc. 3rd World Conf. Photovolt. Energy Convers.*, 2003, pp. 2243–2246.

[33] E. Skoplaki, A. G. Boudouvis, and J. A. Palyvos, "A simple correlation for the operating temperature of photovoltaic modules of arbitrary mounting," *Sol. Energy Mater. Sol. Cells*, vol. 92, no. 11, pp. 1393–1402, 2008.

[34] J. A. Duffie and W. A. Beckman, *Solar Engineering of Thermal Processes,* 4th ed. Hoboken, NJ, USA: Wiley, 2013.

[35] A. Barange and V. Sharma, "Maximum power point tracking for photovoltaic systems," *Int. Res. J. Eng. Technol.*, vol. 6, pp. 604–608, 2019.

[36] P. J. Pérez-Higueras, P. Rodrigo, E. F. Fernández, F. Almonacid, and L. Hontoria, "A simplified method for estimating direct normal solar irradiation from global horizontal irradiation useful for CPV applications," *Renewable Sustain. Energy Rev.*, vol. 16, no. 8, pp. 5529–5534, 2012.

[37] National Standards Authority of Ireland, "Photovoltaic devices—Part 5: Determination of the equivalent cell temperature (ECT) of photovoltaic (PV) devices by the open-circuit voltage method," *Int. Electr. Commission*, Geneva, Switzerland, IEC 60904-5, Ed. 2.0, 2011.

[38] M. D. Yandt *et al.*, "Estimating cell temperature in a concentrating photovoltaic system," in *Proc. AIP Conf.*, 2012, pp. 172–175.

[39] W. Durisch, B. Bitnar, J. Mayor, H. Kiess, K. Lam, and J. Close, "Efficiency model for photovoltaic modules and demonstration of its application to energy yield estimation," *Sol. Energy Mater. Sol. Cells*, vol. 91, no. 1, pp. 79–84, 2007.

[40] M. Topi, K. Brecl, and J. Sites, "Effective efficiency of PV modules under field conditions," *Prog. Photovolt. Res. Appl.*, vol. 15, no. 1, pp. 19–26, 2007.

[41] S. C. W. Krauter, "Development of an integrated solar home system," *Sol. Energy Mater. Sol. Cells*, vol. 82, no. 1/2, pp. 119–130, 2004.

[42] J. D. Mondol, Y. G. Yohanis, M. Smyth, and B. Norton, "Long-term validated simulation of a building integrated photovoltaic system," *Sol. Energy*, vol. 78, no. 2, pp. 163–176, 2005.

[43] J. D. Mondol, Y. G. Yohanis, and B. Norton, "Comparison of measured and predicted long term performance of grid a connected photovoltaic system," *Energy Convers. Manage.*, vol. 48, no. 4, pp. 1065–1080, 2007.

[44] T. Hove, "A method for predicting long-term average performance of photovoltaic systems," *Renewable Energy*, vol. 21, no. 2, pp. 207–229, 2000.

[45] G. N. Tiwari, *Solar Energy: Fundamentals, Design, Modelling, and Applications.* Oxford, U.K.: Alpha Science Int'l. Ltd, 2002.

[46] U. Eicker, *Solar Technologies for Buildings*. Hoboken, NJ, USA: Wiley, 2006.

[47] G. M. Tina and R. Abate, "Experimental verification of thermal behaviour of photovoltaic modules," in *Proc. 14th IEEE Mediterranean Electrotechnical Conf.*, 2008, pp. 579–584.

[48] T. Markvart, *Solar Electricity*, vol. 6. Hoboken, NJ, USA: Wiley, 2000.

[49] S. Diaf, G. Notton, M. Belhamel, M. Haddadi, and A. Louche, "Design and techno-economical optimization for hybrid PV/wind system under various meteorological conditions," *Appl. Energy*, vol. 85, no. 10, pp. 968–987, 2008.

[50] L. Castaner and S. Silvestre, *Modelling Photovoltaic Systems Using PSpice*. Hoboken, NJ, USA: Wiley, 2002.

[51] C. Schwingshackl *et al.*, "Wind effect on PV module temperature: Analysis of different techniques for an accurate estimation," *Energy Procedia*, vol. 40, pp. 77–86, 2013.

[52] J. D. Mondol, Y. G. Yohanis, and B. Norton, "The effect of low insolation conditions and inverter oversizing on the long-term performance of a grid-connected photovoltaic system," *Prog. Photovolt. Res. Appl.*, vol. 15, no. 4, pp. 353–368, 2007.

[53] S. Tselepis and Y. Tripanagnostopoulos, "Economic analysis of hybrid photovoltaic/thermal solar systems and comparison with standard PV modules," in *Proc. Int. Conf. PV Eur.*, 2002, pp. 7–11.

[54] A. Tiwari, M. S. Sodha, A. Chandra, and J. C. Joshi, "Performance evaluation of photovoltaic thermal solar air collector for composite climate of India," *Sol. Energy Mater. Sol. Cells*, vol. 90, no. 2, pp. 175–189, 2006.

[55] M. M. Rahman, M. Hasanuzzaman, and N. A. Rahim, "Effects of various parameters on PV-module power and efficiency," *Energy Convers. Manag.*, vol. 103, pp. 348–358, 2015.

[56] S. Dubey and G. N. Tiwari, "Thermal modeling of a combined system of photovoltaic thermal (PV/T) solar water heater," *Sol. Energy*, vol. 82, no. 7, pp. 602–612, 2008.

[57] S. Dubey and A. A. O. Tay, "Testing of two different types of photovoltaic-thermal (PVT) modules with heat flow pattern under tropical climatic conditions," *Energy Sustain. Develop.*, vol. 17, no. 1, pp. 1–12, 2013.

[58] F. Almonacid, P. J. Pérez-Higueras, E. F. Fernández, and P. Rodrigo, "Relation between the cell temperature of a HCPV module and atmospheric parameters," *Sol. Energy Mater. Sol. Cells*, vol. 105, pp. 322–327, 2012.

[59] R. Chenni, M. Makhlouf, T. Kerbache, and A. Bouzid, "A detailed modeling method for photovoltaic cells," *Energy*, vol. 32, no. 9, pp. 1724–1730, 2007.

[60] A. M. Muzathik, "Photovoltaic modules operating temperature estimation using a simple correlation," *Int. J. Energy Eng.*, vol. 4, no. 4, pp. 151–158, 2014.

[61] E. Akyuz, C. Coskun, Z. Oktay, and I. Dincer, "A novel approach for estimation of photovoltaic exergy efficiency," *Energy*, vol. 44, no. 1, pp. 1059–1066, 2012.

[62] F. Rubio, M. Martinez, R. Coronado, J. L. Pachón, and P. Banda, "Deploying CPV power plants-ISFOC experiences," in *Proc. 33rd IEEE Photovolt. Specialists Conf.*, 2008, pp. 1–4.

[63] D. Faiman, "Assessing the outdoor operating temperature of photovoltaic modules," *Prog. Photovolt. Res. Appl.*, vol. 16, no. 4, pp. 307–315, 2008.

[64] S. Kurtz *et al.*, "Evaluation of high-temperature exposure of rack-mounted photovoltaic modules," in *Proc. 34th IEEE Photovolt. Specialists Conf.*, 2009, pp. 2399–2404.

[65] T. Hornung, M. Steiner, and P. Nitz, "Estimation of the influence of fresnel lens temperature on energy generation of a concentrator photovoltaic system," *Sol. Energy Mater. Sol. Cells*, vol. 99, pp. 333–338, 2012.

[66] H. Bahaidarah, S. Rehman, A. Subhan, P. Gandhidasan, and H. Baig, "Performance evaluation of a PV module under climatic conditions of Dhahran, Saudi Arabia," *Energy Exploration Exploitation*, vol. 33, no. 6, pp. 909–929, 2015.

[67] M. Mattei, G. Notton, C. Cristofari, M. Muselli, and P. Poggi, "Calculation of the polycrystalline PV module temperature using a simple method of energy balance," *Renewable Energy*, vol. 31, no. 4, pp. 553–567, 2006.

[68] P. Hersch and K. Zweibel, "Basic photovoltaic principles and methods," Solar Energy Research Inst., Golden, CO, USA, Tech. Rep.SERI/SP-290-1448, 1982, doi: 10.2172/5191389.

[69] J. S. Griffith, M. S. Rathod, and J. Paslaski, "Some tests of flat plate photovoltaic module cell temperatures in simulated field conditions," in *Proc. 15th Photovolt. Specialists Conf.*, 1981, pp. 822–830. [Online]. Available: https://ui.adsabs.harvard.edu/abs/1981pvsp.conf.822G

[70] O. M. Tzuc, A. Bassam, P. E. Mendez-Monroy, and I. S. Dominguez, "Estimation of the operating temperature of photovoltaic modules using artificial intelligence techniques and global sensitivity analysis: A comparative approach," *J. Renewable Sustain. Energy*, vol. 10, no. 3, 2018, Art. no. 33503.

[71] E. L. Maxwell, W. Marion, D. Myers, M. Rymes, S. Wilcox, "National solar radiation data base, vol. 2—Final technical report (1961-1990)," *Nat. Renew. Energy Lab.*, Washington, DC, USA, Rep. NREL/TP-463-5784, 1995, doi: 10.2172/70747.

[72] Meteonorm: Global meteorological database for solar energy and applied climatology. Version 4.0: edition 2000. Meteotest. Software and data on CD-ROM. Switzerland. [Online]. Available: https://meteonorm.com/en/download

[73] M. Muller, C. Deline, B. Marion, S. Kurtz, and N. Bosco, "Determining outdoor CPV cell temperature," in *Proc. AIP Conf.*, 2011, pp. 331–335.

[74] G. Peharz, J. P. F. Rodríguez, G. Siefer, and A. W. Bett, "A method for using CPV modules as temperature sensors and its application to rating procedures," *Sol. Energy Mater. Sol. Cells*, vol. 95, no. 10, pp. 2734–2744, 2011.

[75] M. D. Yandt, J. P. D. Cook, M. Kelly, H. Schriemer, and K. Hinzer, "Dynamic real-time I-v curve measurement system for indoor/outdoor characterization of photovoltaic cells and modules," *IEEE J. Photovolt.*, vol. 5, no. 1, pp. 337–343, Jan. 2015.

[76] M. Al-Addous, Z. Dalala, C. B. Class, F. Alawneh, and H. Al-Taani, "Performance analysis of off-grid PV systems in the Jordan valley," *Renewable Energy*, vol. 113, pp. 930–941, 2017.

[77] W. W. Ma, M. G. Rasul, G. Liu, M. Li, and X. H. Tan, "Climate change impacts on techno-economic performance of roof PV solar system in Australia," *Renewable Energy*, vol. 88, pp. 430–438, 2016.

[78] M. Bardhi, G. Grandi, and G. M. Tina, "Comparison of PV cell temperature estimation by different thermal power exchange calculation methods," in *Proc. Int. Conf. Renewable Energies Power Qual.*, 2012, pp. 28–30.

[79] Seaward, "SolarSurvey 100/200R Series The ultimate solar site-survey tool," Seaward Group USA, Tampa, FL, USA, Rep. 372, 2019.

[80] C. K. Pandey and A. K. Katiyar, "Solar radiation: Models and measurement techniques," *J. Energy*, vol. 2013, 2013, Art. no. 305207.

[81] H. Al-Taani and S. Arabasi, "Solar irradiance measurements using smart devices: A cost-effective technique for estimation of solar irradiance for sustainable energy systems," *Sustainability*, vol. 10, no. 2, pp. 1–11, 2018.

[82] Y. Ota, T. Masuda, K. Araki, and M. Yamaguchi, “A mobile multipyranometer array for the assessment of solar irradiance incident on a photovoltaic-powered vehicle,” *Sol. Energy*, vol. 184, pp. 84–90, 2019.

[83] P. Sinha, W. Hayes, B. Littmann, L. Ngan, and R. Znaidi, “Environmental variables affecting solar photovoltaic energy generation in Morocco,” in *Proc. IEEE Int. Renewable Sustain. Energy Conf.*, 2014, pp. 230–234.

[84] W. Liao, Y. Heo, and S. Xu, “Simplified vector-based model tailored for urban-scale prediction of solar irradiance,” *Sol. Energy*, vol. 183, pp. 566–586, 2019.

[85] J. A. Palyvos, “A survey of wind convection coefficient correlations for building envelope energy systems’ modeling,” *Appl. Thermal Eng.*, vol. 28, no. 8/9, pp. 801–808, 2008.

[86] F. Romary, A. Caldeira, S. Jacques, and A. Schellmanns, “Thermal modelling to analyze the effect of cell temperature on PV modules energy efficiency,” in *Proc. IEEE 14th Eur. Conf. Power Electron. Appl.*, 2011, pp. 1–9.

[87] A. Finamore, V. Calderaro, V. Galdi, A. Piccolo, and G. Conio, “A day-ahead wind speed prediction based on meteorological data and the seasonality of weather fronts,” in *Proc. IEEE PES GTD Gd Int. Conf. Expo. Asia*, 2019, pp. 915–920.

[88] A. F. G. Silva, E. L. Zaparoli, and C. R. Andrade, “Least squares fitting of computational fluid dynamics results to measured vertical wind profiles,” *J. Sol. Energy Eng.*, vol. 139, no. 3, pp. 1–13, 2017.

[89] A. Abiola-Ogedengbe, H. Hangan, and K. Siddiqui, “Experimental investigation of wind effects on a standalone photovoltaic (PV) module,” *Renewable Energy*, vol. 78, pp. 657–665, 2015.

[90] R. I. S. Pereira, M. M. Camboim, A. W. R. Villarim, C. P. Souza, S. C. S. Jucá, and P. C. M. Carvalho, “On harvesting residual thermal energy from photovoltaic module back surface,” *AEU- Int. J. Electron. Commun.*, vol. 111, 2019, Art. no. 152878.

[91] E. S. Zimmerman and L. R. Hartwick, “Ambient temperature monitoring technique,” U.S. Patent 5001 656, Mar. 1991.

[92] K. Kawajiri, T. Oozeki, and Y. Genchi, “Effect of temperature on PV potential in the world,” *Environ. Sci. Technol.*, vol. 45, no. 20, pp. 9030–9035, 2011.

[93] P. Singh and N. M. Ravindra, “Temperature dependence of solar cell performance-an analysis,” *Sol. Energy Mater. Sol. Cells*, vol. 101, pp. 36–45, 2012.

[94] V. Salas, E. Olias, A. Barrado, and A. Lazaro, “Review of the maximum power point tracking algorithms for stand-alone photovoltaic systems,” *Sol. Energy Mater. Sol. Cells*, vol. 90, no. 11, pp. 1555–1578, 2006.

[95] O. Dupré, R. Vaillon, and M. A. Green, “Temperature coefficients of photovoltaic devices,” in *Thermal Behavior Photovoltaic Devices*, Berlin, Germany: Springer, 2017, pp. 29–74.

[96] L. Bergman and A. S. Lavine, *Fundamentals of Heat and Mass Transfer*, 7th ed. Hoboken, NJ, USA: Wiley, 2011.

[97] L. M. R. Ospina, “Modelagem e análise de um coletor fotovoltaico térmico,” M.S. thesis, Mech. Eng. Dept., Pernambuco Federal Univ., Recife, PE, Brazil, 2016.

[98] T. T. Chow, “Performance analysis of photovoltaic-thermal collector by explicit dynamic model,” *Sol. Energy*, vol. 75, no. 2, pp. 143–152, 2003.

[99] E. Skoplaki and J. A. Palyvos, “On the temperature dependence of photovoltaic module electrical performance: A review of efficiency/power correlations,” *Sol. Energy*, vol. 83, no. 5, pp. 614–624, 2009.

[100] M. P. Chaves, I. M. Dupont, P. C. M. Carvalho, and D. N. Araujo, “Estudo sobre sombreamento em planta fotovoltaica localizada em zona urbana de Fortaleza-CE,” *Revista Tecnologia*, vol. 40, no. 1, pp. 1–21, 2019, doi: 10.5020/23180730.2019.8898.

[101] D. N. Araújo, P. C. M. de Carvalho, and I. M. Dupont, “Efeitos da acumulação de sujeira sobre o desempenho de módulos fotovoltaicos,” *Revista Tecnologia*, vol. 40, no. 2, pp. 1–23, 2019, doi: 10.5020/23180730.2019.9414.

[102] S. Gallardo-Saavedra, L. Hernández-Callejo, and O. Duque-Perez, “Technological review of the instrumentation used in aerial thermographic inspection of photovoltaic plants,” *Renewable Sustain. Energy Rev.*, vol. 93, pp. 566–579, 2018.

[103] *Solar PV Panel Operational Theory*, 2020. [Online]. Available: https://www.infraredimagingservices.com/solar-panel/

[104] X. Ju, A. Vossier, Z. Wang, A. Dollet, and G. Flamant, “An improved temperature estimation method for solar cells operating at high concentrations,” *Sol. Energy*, vol. 93, pp. 80–89, 2013.

[105] K. Nishioka, K. Miyamura, Y. Ota, M. Akitomi, Y. Chiba, and A. Masuda, “Accurate measurement and estimation of solar cell temperature in photovoltaic module operating in real environmental conditions,” *Jpn. J. Appl. Phys.*, vol. 57, no. 8S3, 2018, Art. no. 08RG08.